A NOVEL APPROACH FOR NOISE REDUCTION IN THE GABOR TIME-FREQUENCY DOMAIN

Behnaz Pourebrahimi and Jan C. A. van der Lubbe
ICT Group, EEMCS Faculty, Delft University of Technology, The Netherlands

Keywords: Noise reduction, Time-frequency transform, Gabor transform, Low-pass filter, Image features.

Abstract: In this paper, a noise reduction technique is introduced based on the Gabor time-frequency transform. In the proposed approach, noise is removed using low pass filters locally in the transform domain. Finding the cut-off frequency for the low pass filters in such a way that image does not loose its features, is an important issue. The optimal cut-off frequency of the low pass filters are computed in an iterative method for each sub-block of the image. The followed approach, besides showing a good performance in removing noise, it also performs well in preserving image features.

1 INTRODUCTION

In the literature, there are several image denoising methods which are applied in spatial, transform, or time-frequency domains (Buades et al., 2004)(Barthel et al., 2003),(Wang et al., 2006).(Cristobal et al., 1996). In the spatial domain a small mask is convolved with the image. This mask can be an averaging filter, a mean or Gaussian filter. In the transform domain, first the image is translated to the transform domain, then it is multiplied by a low pass filter and at the end by the inverse transformation, the enhanced image is obtained. In the transform domain, noise in the grey levels of an image contributes heavily to the high frequency components and the most of the image energy is concentrated in the low frequency components. Although, applying a low pass filter to a noisy image in the transform domain reduces the noise, at the same time it could eliminate some high frequency components that are not related to noise and weaken sharp transitions like edges. Furthermore, the transforms which perform on the whole image, do not take into account any spatial information where the frequency components come from. Therefore, noise reduction by low pass filtering in such domains does not preserve the local information of the image very well. Time-frequency transforms combine time-domain and frequency-domain analysis and allow obtaining a revealing picture of the temporal localization of the signal's spectral components.

In this paper, we consider the Gabor time-frequency transform (Gabor, 1946) as a noise reduction technique. The Gabor transform is considered as the optimum case of the short time Fourier transform (STFT) in which the window function is chosen to have a Gaussian shape. This choice of the window function in the 2-D Gabor elementary functions guarantees the lower bound of the joint uncertainty (i.e. the 2-D Heisenberg inequality) in the two conjoint spatial-frequency domains. We propose an algorithm in which noise is suppressed by applying low pass filters to Gabor coefficients locally. The algorithm by finding the optimal cut-off frequencies for low pass filters attempts to preserve local information of the image. We compare the performance of our approach with two Gaussian and Kuwahara filters given their optimal performances. We also compare our algorithm with a wavelet based denoising method. The results show a good performance of our approach regarding the noise suppression and also preserving the image features like edges.

The paper is structured as follows. Section 2 gives an overview of 2D Gabor transform. We discuss noise reduction in the Gabor domain and introduce our method in Section 3. The results of applying our method to noisy Lena image and comparison with other methods are presented in Section 4. Finally, we conclude in Section 5.

2 2D DISCRETE GABOR TRANSFORM

The Gabor transform is first proposed by Gabor (Gabor, 1946) for one-dimensional signals to analyze

Pourebrahimi B. and C. A. van der Lubbe J. (2009).
A NOVEL APPROACH FOR NOISE REDUCTION IN THE GABOR TIME-FREQUENCY DOMAIN.
In *Proceedings of the Fourth International Conference on Computer Vision Theory and Applications*, pages 22-27
DOI: 10.5220/0001768000220027

speech and audio signals and later extended by Daugman (Daugman, 1985) to two-dimensions. The Gabor analysis is based on projecting a given signal/image onto a family of shifted and modulated Gaussian window functions, which are called the "Gabor elementary functions" or the "Gabor basis functions". The corresponding projection coefficients are called the "Gabor transform coefficients". The use of such a transform is motivated by the fact that Gabor elementary functions have an optimal localization property, in the joint time (or spatial) and frequency domains. This leads to optimal extraction of the textural information from the images, which is an important feature for pattern recognition, segmentation, and image analysis applications. Beside the optimal localization property other benefits of the Gabor transform include compatibility with the human visual system and energy packing capability, which leads to lower entropy in the transform domain.

As proposed by Daugman (Daugman, 1988) for image compression and analysis, the elementary functions are described in the following manner:

$$G(x,y) = \exp(-\pi[(x-x_0)^2\alpha^2 + (y-y_0)^2\beta^2]) \times \exp(-2\pi * i[u_0(x-x_0) + v_0(y-y_0)]). \quad (1)$$

where (x_0, y_0) are the spatial coordinates of the center and (u_0, v_0) are the spatial frequency parameters. α and β are the standard deviations of the elliptical Gaussian along x and y. The deficiency of the Gabor transform, is that the elementary functions are not orthogonal. Therefore, there is no straightforward method available for extracting these transform coefficients. If they were orthogonal, the extraction of these coefficients could have been done easily by taking the simple inner product. Many approaches have been proposed to find a method for extracting the Gabor transform coefficients. In this paper, we use the algorithm introduced in (Teuner and Hosticka, 1993) to compute the Gabor coefficients. This algorithm is essentially an FFT-based gradient descent approach.

Consider a discrete two-dimensional signal $I(x,y)$, such as a digitized image of size $P * Q$. The image is divided into sub-images, each with $M * N$ pixels and centers located at $x_m, y_n = mM, nN$ for integers (m,n). The elementary functions, whose widths are determined by the Gaussian envelope parameters α and β in equation (1), are defined over a $2M * 2N$ spatial lattice cell. A complete set of Gabor elementary functions is defined for each sub-image (m,n) by varying the spatial frequencies $\{u_r, v_s\} = \left\{\frac{r}{2M}, \frac{s}{2N}\right\}$ corresponding to the $2M * 2N$ spatial lattice cell. The parameter r and s take on even integer values, $r = 0, 2, 4, ..., 2M-2$ and $s = 0, 2, 4, ..., 2N-2$, because the sub-image size is M*N. The center of each elementary function coincides with that of a sub-image and (1) can now be rewritten as:

$$G_{mnrs}[x,y] = \exp(-\pi[(x-mM)^2\alpha^2 + (y-nN)^2\beta^2]) \times \exp(-2\pi i[\frac{r(x-mM)}{2M} + \frac{s(y-nN)}{2N}]). \quad (2)$$

Each Gabor elementary function is now uniquely determined by the integer pairs (m,n) and (r,s) representing the spatial center and frequency parameters, respectively (Srinivasan et al., 1993). The Gabor transform of a 2-D image can now be written as:

$$I(x,y) = \sum_m \sum_n \sum_r \sum_s C_{mnrs} G_{mnrs} \quad (3)$$

where C_{mnrs} are Gabor coefficients. If there would exist the functions W_{mnrs} that were orthogonal to G_{mnrs}, then the Gabor coefficients would be computed as follows :

$$C_{mnrs} = \sum_{x=0}^{P-1} \sum_{y=0}^{Q-1} I(x,y) W_{mnrs}(x,y). \quad (4)$$

where

$$W_{mnrs} = W(x-mM, y-nN) e^{-2\pi j\left(\frac{rx}{M} + \frac{sy}{N}\right)}. \quad (5)$$

and below equation shows the orthogonality condition:

$$\sum_{x=0}^{P-1} \sum_{y=0}^{Q-1} W_{mnrs}(x,y) G_{mnrs}(x,y) = \delta_m \delta_n \delta_r \delta_s. \quad (6)$$

Equation (4) can be presented as follows:

$$C_{mnrs} = \sum_{x=0}^{P-1} \sum_{y=0}^{Q-1} [I(x,y) W(x-mM, y-nN)] e^{-2\pi j\left(\frac{rx}{M} + \frac{sy}{N}\right)} = \sum_{x=0}^{P-1} \sum_{y=0}^{Q-1} I'(x,y) e^{-2\pi j\left(\frac{rx}{M} + \frac{sy}{N}\right)}. \quad (7)$$

The signal $I'(x,y)$ can be interpreted as an image $I(x,y)$ windowed by localized Gaussian, which is centered at the location (m,n) on the Gabor lattice. If M and N are powers of two, and the width P and the height Q of the array (x,y) are multiple integers of M and N, the computation of (7) requires a $P * Q$ 2-D FFT. With substitution $D_m = \frac{P}{M}$ and $D_n = \frac{Q}{N}$,equation (7) can be modified as follows:

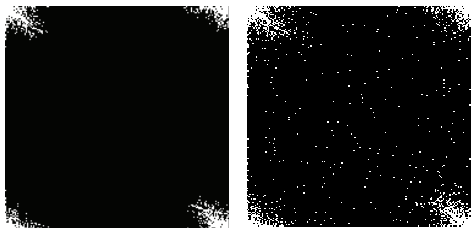

(a) **(b)**

Figure 1: Power spectrum of an original image (a) and a noisy image (b) in the Gabor domain.

$$\begin{aligned}
\sum_{x=0}^{P-1}\sum_{y=0}^{Q-1} I^{'}(x,y)e^{-2\pi j(\frac{rx}{M}+\frac{sy}{N})} &= \sum_{x=0}^{M-1}\sum_{y=0}^{N-1} I^{'}(x,y)e^{-2\pi j(\frac{rx}{M}+\frac{sy}{N})} \\
&+ \sum_{x=M}^{2M-1}\sum_{y=0}^{N-1} I^{'}(x,y)e^{-2\pi j(\frac{rx}{M}+\frac{sy}{N})} \\
&+ \sum_{x=0}^{M-1}\sum_{y=N}^{2N-1} I^{'}(x,yt)e^{-2\pi j(\frac{rx}{M}+\frac{sy}{N})} + \ldots \\
&+ \sum_{x=M(D_m-1)}^{D_mM-1}\sum_{y=N(D_n-1)}^{D_nN-1} I^{'}(x,y)e^{-2\pi j(\frac{rx}{M}+\frac{sy}{N})} \\
&= \sum_{x=0}^{M-1}\sum_{y=0}^{N-1} I^{'}(x,y)e^{-2\pi j(\frac{rx}{M}+\frac{sy}{N})} \\
&+ \sum_{x=0}^{M-1}\sum_{y=0}^{N-1} I^{'}(x+M,y)e^{-2\pi j(\frac{rx}{M}+\frac{sy}{N})} \\
&+ \sum_{x=0}^{M-1}\sum_{y=0}^{N-1} I^{'}(x,y+N)e^{-2\pi j(\frac{rx}{M}+\frac{sy}{N})} + \ldots \\
&+ \sum_{x=0}^{M-1}\sum_{y=0}^{N-1} I^{'}(x+(D_m-1)M,y+(D_n-1)N)e^{-2\pi j(\frac{rx}{M}+\frac{sy}{N})} \\
&= \sum_{x=0}^{M-1}\sum_{y=0}^{N-1}[\sum_{D_m=0}^{M-1}\sum_{D_n=0}^{N-1} I^{'}(x+D_mM,y+D_nN)]e^{-2\pi j(\frac{rx}{M}+\frac{sy}{N})}.
\end{aligned} \tag{8}$$

Hence FFT of an $P*Q$ image $I^{'}(x,y)$ followed by decimation is substituted by $M*N$ point FFT, where the FFT input signal $I^{'}(x,y)$ is calculated by summing all points , equidistantly spaced about M and N. Reconstruction of the image can be done in the same way by Gabor coefficients.

3 NOISE REDUCTION IN GABOR TRANSFORM DOMAIN

In the Gabor domain, most energy of the image is concentrated in a few coefficients. With computing the Gabor transform of a N*N image using a N*N Gaussian window, we observe that most of the image energy has been concentrated in the low frequencies. Figure 1 shows the image spectrum of an image without noise and the corresponding noisy image in the Gabor transform domain. From the figure 1(a), we can see that the energy compaction of the image spectrum is concentrated in the low frequency components, while in a noisy image (figure 1(b)) energy compaction is expanded in the whole image transform domain. This energy packing property in Gabor domain can be used for noise suppression. Such as, eliminating high frequency components in transform domain reduces the noise without loosing the image information in low frequency components. A low pass filter can eliminate the high frequency components. Selecting the cut-off frequency of low pass filter is important to make sure that no components belonging to the image information is removed.

Figure 2 shows a $N*N$ low pass filter, chosen in the Gabor domain. The low pass filter is selected according to energy compaction of a $N*N$ image block in the Gabor domain. The components in the dashed area contain the most energy of the block. In this figure, x detects the harmonic border of the image spectrum. These regions have been chosen based on conjugated coefficients that have the same absolute values.

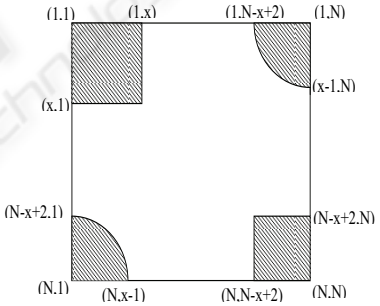

Figure 2: Low pass filter.

3.1 Proposed Noise Reduction Algorithm

In this section, we introduce our noise reduction algorithm. In the Gabor transform domain, the image is analyzed through a Gaussian window whose dimensions are smaller than the dimension of the image. As already discussed, energy compaction of an image in the Gabor domain is concentrated in the low frequency components. So energy compaction in high frequency components is related to noise. Using a low-pass filter, we can save low frequency components and eliminate the rest. Low pass filtering is performed in the following manner: the Gaussian window is moved over the image and the Gabor transform of the sub-image inside the window is calculated. Ga-

bor components of the sub-image are filtered by a low pass filter. Then by an inverse Gabor transform, the enhanced sub-image is obtained. This procedure continues till the whole image is covered.

We assume that the dimension of the Gaussian window is $m*m$. cf is considered as the cut-off frequency of the low-pass filter. The cut-off frequency cf for each sub-image is calculated based on the maximum peak signal-to-noise ratios between different versions of the enhanced sub-images with different cut-off frequencies. We assume that the optimal cut-off frequency is achieved when the peak signal-to-noise ratio has its maximum value. Considering this assumptions, the algorithm works as follows:

1. The Gaussian window is located at the coordinates $(1,1)$ of the image.
2. The block of the image inside the window is named as x. Sub-image x is transformed to the Gabor domain.
3. Cut-off frequency cf is initialized to $cf = 1$ and variable $psnr = 0$ is set ($psnr$: peak signal-to-noise ratio).
4. Gabor coefficients from step 2 are filtered by a low-pass filter with the cut-off frequency cf.
5. Inverse Gabor transform is performed on the filtered Gabor coefficients obtained from step 4 (the new enhanced sub-image is named ex).
6. The peak signal-to-noise ratio ($psnr$) for two sub-images x and ex are computed.
7. Cut-off frequency is increased ($cf = cf + 1$). The variable x is replaced with ex ($x = ex$). The steps 4-6 are repeated while $cf < m/2 - 1$.
8. The sub-image ex (from step 5) is selected as the enhanced version of the original sub-image when $psnr$ has its maximum value ($psnr$(s) are computed in step 6).
9. The Gaussian window is moved horizontally along the image by f pixels ($1 < f < m$).
10. The values of the pixels in the overlapped areas of the moving window are computed by averaging.
11. If end of the row is reached by the window, then the window is moved vertically along the image by f pixels (starting from left side of the image).
12. If the whole image is covered then the algorithm stops, otherwise goes to step 2.

Table 1: Peak Signal to Noise Ratio (PSNR) in different methods with two levels of Gaussian noise.

	PSNR σ_N=25	PSNR σ_N=50
Noisy Image	20.16	14.14
Enhanced Image (Gabor)	27.92	25.37
Enhanced Image (Kuwahara)	26.44	23.80
Enhanced Image (Gaussian)	28.91	26.41

4 PERFORMANCE EVALUATION

To evaluate the performance of our noise reduction algorithm, we consider Lena image and apply the noise reduction technique to its noisy version. The noisy image shown in figure 3(a) has been corrupted by the Gaussian noise with variance $\sigma = 25$. We compare the performance of our approach with Gaussian and Kuwahara filters. For each approach, we measure the peak signal-to-noise ratio (PSNR) between the original and enhanced image. The PSNR is calculated based on the mean square error (MSE) between the original and the enhanced image:

$$MSE = \frac{1}{M*N}\sum_{i=1}^{M}\sum_{j=1}^{N}(I(i,j)-K(i,j))^2 \quad (9)$$

$$PSNR = 10\log_{10}(\frac{p^2}{MSE}) \quad (10)$$

where I and K are the original and the noisy version of an image with dimension $M \times N$ and p is the maximum possible pixel value of the image.

For our approach (in section 3.1), we applied the algorithm with different sizes of the windows (m) and different overlap values (f). We observed that the best value for windows overlap is $f = m/2$. By applying different sizes of windows, the best performance was achieved for $m = 16$ and $f = 8$ in the most cases.

We considered a Kuwahara filter with the size 5×5. The Kuwahara filter is an edge-preserving filter that smooths the noisy image but attempts to preserve edges. With Gaussian filter, we tested with different values for sigma. The results of applying the Gaussian filter shown in this paper are the ones which have given the highest peak signal-to-noise ratio (PSNR).

Table 2: Signal to Noise Ratio (SNR) in different methods with three levels of Gaussian noise.

	SNR σ_N=15	SNR σ_N=20	SNR σ_N=25
Noisy Image	18.75	16.25	14.29
Enhanced Image (Gabor)	24.02	22.92	22.06
Enhanced Image (WFW)	23.79	21.71	20.08

The enhanced images provided by applying the three methods are shown in figure 3. The peak signal-

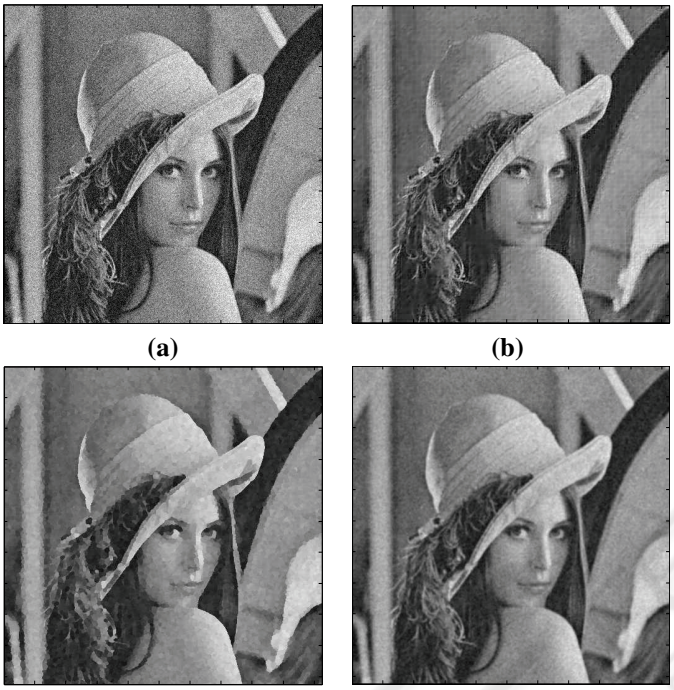

Figure 3: (a)Noisy image (Gaussian noise $\sigma = 25$), (b)Enhanced image using proposed algorithm (m=16, f=8), (c)Enhanced image using Kuwahara filter (size=5×5), (d)Enhanced image using Gaussian filter.

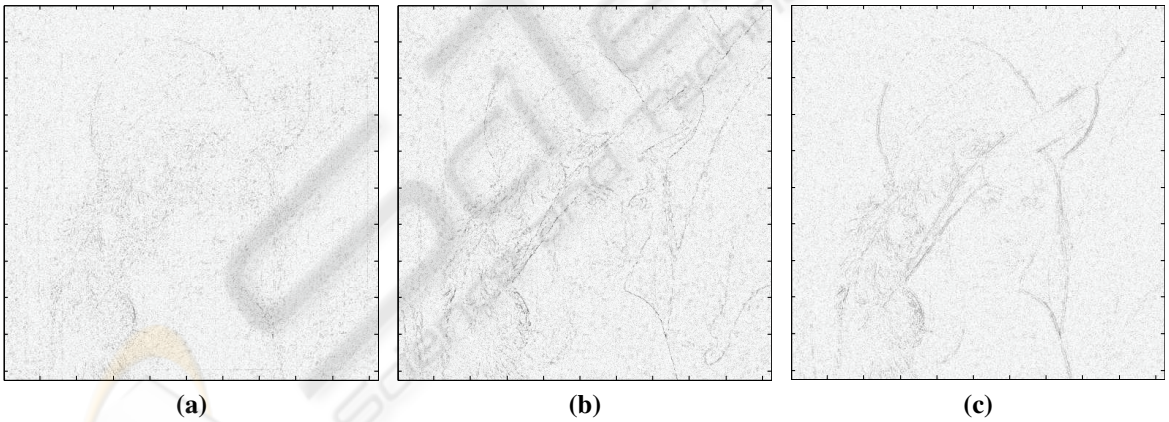

Figure 4: Difference between noisy image and its enhanced version; (a)applying our method, (b)applying Kuwahara filter, (c)applying Gaussian filter.

to-noise ratio (PSNR) is measured in each case and is presented in table 1. Considering PSNR(s) in different approaches, the Gaussian filter shows the highest PSNR and Kuwahara filter the lowest. Let us remark that the presented enhanced images with applying Gaussian and Kuwahara filters are selected given the highest PSNR.

It should be taken into account that a higher PSNR does not always guarantee a good visual quality of the restored image. The PSNR by itself would not be meaningful and the visual quality of the restored image is also necessary to evaluate the performance of denoising methods. To compare visual quality of the enhanced images, we consider the subtraction of enhanced image from its noisy version. The more this difference looks like a real Gaussian noise, the better the method is. In fact, this difference tells us which geometrical features or details are preserved

by the denoising process and which are eliminated. Figures 4(a), 4(b) and 4(c) depict the difference between the noisy image and the denoised image using our approach, Kuwahara and Gaussian approaches respectively. The results show that our method preserve more image features such as edges compared to other two approaches. As, the difference of the noisy and the enhanced image in our approach looks more like Gaussian noise and contains less image features.

In the results shown above, we compared our algorithm with two methods in spatial domain. In following, we compare our method with a wavelet based denoising approach in time-frequency domain. We use the results of the Wiener Filtering in the Wavelet domain (WFW) on noisy Lena image with different level of Gaussian noise presented in (Wang et al., 2006). As in this paper the results are shown based on measuring signal-to-noise ratio (SNR), we also compute the SNR when applying our method to the noisy image with the same level of Gaussian noise. SNR is computed as follows:

$$SNR = 10\log_{10}\left(\frac{\sum_{i=1}^{M}\sum_{j=1}^{N} S_0(i,j)^2}{\sum_{i=1}^{M}\sum_{j=1}^{N}(S_0(i,j)-S(i,j))^2}\right) \quad (11)$$

where S_0 is the noise free signal and S is the denoised signal (Wang et al., 2006). Table 2 shows the results for the two approaches. From the results, we can see the our approach is also outperforming Wiener filter in the wavelet domain. Our approach gives higher signal-to-noise ratio for different level of noise.

5 CONCLUSIONS

In this paper, we have introduced a method for noise suppressing in the Gabor time-frequency domain. In the transform domain, high frequency components are corresponding to the noise in the image. Considering this fact, the approach attempts to eliminate noise with the low-pass filters which are located in the spatial domain. In this way, the local information of the image are preserved. The results of applying our approach to the noisy Lena image show good performance compared with the spatial denoising methods as well as a denoising method in the time-frequency domain. The enhanced image provided by our approach, besides removing noise, shows a better quality in preserving image features compared to the approaches in the spatial domain.

REFERENCES

Barthel, K. U., Cycon, H. L., and Marpe, D. (2003). Image denoising using fractal and wavelet-based methods. In *SPIE Proc*, pages 10–18.

Buades, A., Coll, B., and Morel, J. M. (2004). On image denoising methods. Technical report, Technical Note, CMLA (Centre de Mathematiques et de Leurs Applications.

Cristobal, G., Chagoyen, M., Escalante-Ramirez, B., and Lopez-Miranda, J. (1996). Wavelet-based denoising methods. a comparative study with applications in microscopy. In *SPIE Proc. Wavelet Applications in Signal and Image Processing IV*, volume 2825, pages 660–671.

Daugman, J. G. (1985). Uncertainty relation for resolution in space, spatial frequency, and orientation optimized by two-dimensional visual cortical filters. *J. Opt. Soc. Am. A*, 2(7):1160.

Daugman, J. G. (1988). Complete discrete 2-d gabor transforms by nearal networks for image analysis and compression. *IEEE Trans. Acoustics, Speech and Signal Proc.*, 36(7):1169–1179.

Gabor, D. (1946). Theory of communication. 93:429–457.

Srinivasan, V., Bhatia, P., and Ong, S. H. (1993). A fast implementation of the discrete 2-d gabor transform. *Signal Process.*, 31(2):229–233.

Teuner, A. and Hosticka, B. J. (1993). Adaptive gabor transformation for image processing. *IEEE Transactions on Image Processing*, 2(1):112–117.

Wang, Z., Qu, C., and Cui, L. (2006). Denoising images using wiener filter in directionalet domain. In *CIMCA '06: Proceedings of the International Conference on Computational Inteligence for Modelling Control and Automation and International Conference on Intelligent Agents Web Technologies and International Commerce*, page 228, Washington, DC, USA. IEEE Computer Society.